11

Electroretinogram Assessment of Dark Adaptation and Rod Phototransduction from the Central Retina of Japanese Macaques with Dominantly Inherited Drusen

Brett G Jeffrey[1,4], Catherine W Morgans[2,5], Robert M Duvoisin[3,5] and Martha Neuringer[2,4,5]
[1]*Ophthalmic Genetics and Visual Function Branch National Eye Institute, Bethesda, MD*
[2]*Casey Eye Institute*
[3]*Department of Physiology and Pharmacology*
[4]*Oregon National Primate Research Center*
[5]*Oregon Health and Science University, Portland Oregon USA*

1. Introduction

The central retina of humans, apes and monkeys is uniquely characterized amongst mammals by the presence of the macula, a distinct and specialized area 6 mm in diameter (≈22 degrees of visual angle) centered on the fovea (Curcio et al., 2000). The fovea which measures just 0.8 mm and contains the highest photoreceptor and RPE densities in the retina, enables the high visual acuities achieved by primates. A defining characteristic of the macula includes the presence of the xanthophyll pigments, lutein and zeaxanthin, which give the macula its distinctive yellow color (Snodderly et al., 1984). Within the macula, rods outnumber cones by 9:1, lower than the 20:1 rod to cone ratio found for the retina as a whole (Curcio et al., 2000). Therefore, while the macula is cone enriched compared with the peripheral retina, rods are the predominant photoreceptor. In primates, the macula is surrounded by the "rod ring", an area with a radius of approximately 10 to 25 degrees, which contains the highest rod density within the retina (Curcio et al., 1990; Packer et al., 1989; Wikler et al., 1990). For the purposes of the present paper, the central retina is taken to be the area covering 40 degrees of visual angle which encompasses the macula and much of the surrounding rod ring.

With increasing age, changes in retinal morphology include an overall thinning of the retina, accumulation of lipofuscin within the retinal pigment epithelium, thickening of Bruch's membrane, accumulation of basal deposits on and within Bruch's membrane, and accumulation of drusen, the extracellular deposits below the retinal pigment epithelium (Bonilha 2008). The number of photoreceptors within the central and peripheral retina are differentially affected by age. Within the central retina, rod density decreases by 30% between 20 and 90 years of age, while cone density remains constant at the fovea and across

the central retina (Curcio et al., 1993; Gao & Hollyfield 1992). In contrast, cone density in the peripheral retina decreases by 20% between 20 and 90 years of age, while the number of peripheral rods remains constant after 35 years of age (Curcio et al., 1993; Gao & Hollyfield 1992).

Age-related changes in retinal function largely correlate with the morphological changes that occur within the retina with increasing age. Psychophysical studies have documented approximately 35% slowing in the rate of dark adaptation and a 3-fold rise in absolute rod threshold between 20 and 90 years (Jackson et al., 1999). Age-related changes in cone mediated function include reduced contrast sensitivity, lower critical flicker/fusion frequency, poorer color discrimination and lower hyperacuities (Haegerstrom-Portnoy 2005; Wang 2001).

With increasing age, changes observed in both rod and cone ERGs include delays in ERG implicit times, and decreases in ERG a- and b-wave amplitudes (Berrow et al., 2010; Gerth 2009). Aged related changes in phototransduction, measured from the bright flash ERG a-wave, include lower rod sensitivity and slowing of rod inactivation kinetics (Jackson et al., 2006). The changes in psychophysical and ERG functional measures with increasing age cannot be accounted for by changes in optical media properties alone and are therefore, attributable to functional/morphological changes in the retina and/or central nervous system (Morrison, & McGrath 1985; Spear 1993).

Age-related macular degeneration (AMD) is the most common cause of legal blindness in the elderly in the developed world. AMD is a heterogeneous disorder affecting the retinal pigment epithelium/Bruch's membrane complex which results in photoreceptor dysfunction and loss. Early AMD is associated with changes in pigmentation of the retinal pigment epithelium and the presence of soft or confluent drusen in the macula. Signs of advanced AMD include development of geographic atrophy of the retinal pigment epithelium and choroidal neovascularization. AMD is associated with the same changes in retina and retinal pigment epithelium observed with normal aging but in AMD these changes are more marked, progressive and may result in severe visual loss (Bonilha 2008). In AMD, both rod and cone photoreceptors are lost, and photoreceptor density decreases by 30-40% relative to age-matched controls within 0.5 - 3 mm from the fovea (Curcio et al., 1996). Thus the loss of photoreceptors in the paramacular of AMD patients occurs over the same area of maximal rod loss seen in non-pathological aging. Rod death precedes that of cones and there is a greater loss of rods in most AMD patients (Curcio et al., 1996). A recent study, however, reported earlier and more extensive aberrant distribution of opsin immunolabeling compared with rhodopsin in AMD eyes (Shelley et al., 2009). These results suggest that sub-clinical pathological changes may occur earlier in cone photoreceptors than in the rods of AMD eyes.

Psychophysical studies largely support the histopathological evidence of rod and cone photoreceptor loss in early AMD. Cone mediated functions, including flicker and s-cone sensitivities, color vision, temporal contrast, and light adaptation recovery kinetics, are altered in early AMD (Hogg, & Chakravarthy 2006; Neelam et al., 2009; Phipps et al., 2003). Longitudinal studies indicate that some of these parameters alone or in combination may predict those eyes that will progress to more advanced AMD with good specificity and sensitivity (Neelam et al., 2009). Psychophysical studies also support histopathological evidence for greater dysfunction and loss of rods over cones in the parafovea (two to four degrees from the fovea) in early AMD (Neelam et al., 2009). Losses in rod sensitivity precede associated losses in photopic sensitivity and in 87% of AMD patients, the degree of rod

sensitivity loss is greater than for cone sensitivity (Jackson et al., 2002). The time constant of dark adaptation is also markedly delayed in AMD patients (Eisner et al., 1992**;** Haimovici et al., 2002; Owsley et al., 2001). These disturbances of psychophysical function in AMD patients are not limited to the macula but extend across the central retinal area at radii up to 25 to 40 degrees from the fovea, for rod and cone adaptation respectively (Neelam et al., 2009).

ERG assessment of central retinal function in aging and AMD have largely focused on the recording of cone-mediated responses from photopic multifocal (mfERG), focal (fERG) and pattern (pERG) ERGs [Reviewed in (Berrow et al., 2010)]. AMD is associated with delayed implicit times and/or reduction in ERG amplitudes in at least one of the response components of each of these ERG modalities. Drusen are associated with slight delays in mfERG implicit times, although changes are not limited to areas with drusen (Berrow et al., 2010). Correlations between the amplitude of the focal ERG and severity of non-exudative AMD have been reported (Falsini et al., 1999). A focal ERG implementation of the photo stress test also found a significantly slower recovery of bleach cone response in ARM patients (Binns, & Margrain 2007).

Many studies have documented that rhesus macaques develop age related changes in the macula including the formation of drusen and pigmentary changes within the retinal pigment epithelium that are the hallmark of early human AMD (e.g. (Dawson et al., 2008; Gouras et al., 2008)). Like humans, the prevalence and severity of drusen increase with age in rhesus macaques, while some 30% of macaques do not develop drusen at any age (Gouras et al., 2008; Hope et al., 1992) . Drusen do develop earlier in macaques than human and drusen may be observed in up to 53 % of macaques by 10 years of age (Hope et al., 1992), approximately equivalent to 30 human years. Early- and late-onset macular disease has also been reported in a closely related species, the cynomologus macaque (Macaca fascicularis) (Umeda et al., 2005a). Drusen from both macaque species have been confirmed by histopathology to closely resemble human drusen (Gouras et al., 2008). Furthermore, immunohistochemistry and proteonomic studies of isolated drusen from macaques have identified many of the compounds present in human drusen, including apolipoprotein E, complement component C5, membrane cofactor protein and vitronectin (Umeda et al., 2005b). Lastly, rhesus and cynomologus macaques share genetic and nutritional risk factors with human AMD (Francis et al., 2008; Singh et al., 2009; Umeda et al., 2003, Umeda et al., 2005b)

We have identified a distinct retinal disease syndrome that is characterized by dominant inheritance and the early onset of pan-retinal drusen in Japanese macaques (Macaca fuscata) at our Oregon National Primate Research Center (Neuringer M, et al. IOVS 2011;52:ARVO E-Abstract 4008). In a survey of retinal status of 160 of these animals, 42 (26%) showed this disease phenotype. These Japanese macaques are also closely related to the rhesus macaque and we wanted to determine whether the drusen observed in these monkeys were associated with changes in retinal function. Further, given the nature of the photoreceptor changes seen in human AMD, we sought to determine whether central retinal function was selectively altered in these Japanese macaques, particularly as a function of age.

While psychophysical measures of visual function are possible in non-human primates, our experience is that the time involved in training is substantial. Depending of the complexity of the psychophysical task, training may take 6 months to 2 years per animal, making detailed functional examination of a large number of animals prohibitively costly. The widely used full field-electroretinogram (ERG), provides an objective, quick and detailed

assessment of retinal function in non-human primates (e.g (Jeffrey et al., 2002)). However, full field ERG is relatively insensitive to the local structural and functional changes that occur in the central retina in maculopathies such as AMD. Given that rods comprise 90% of macular photoreceptors and that dysfunction and degeneration of rods may precede that of cones with age and in AMD, there is a need for a robust ERG measure of central rod function. Several methods have been used to measure a rod focal ERG for areas ranging from 5 to 40 degrees of the central retina (reviewed in (Binns, & Margrain 2006). The basis of all methods used for obtaining a focal rod ERG is the elimination of the scattered light component generated from the peripheral retina. Sandberg et al (1996) used a subtraction technique to eliminate the stray light component of the double peaked focal flash response. Sandberg's method was extremely time consuming as it required recording full-field ERGs of varying intensity until a response was found that exactly matched amplitude and temporal characteristics of the scattered light response of the focal ERG. The focal response was calculated by subtracting the scattered light response from the original double peaked ERG b-wave response. Other methods used for recording a focal rod-ERG include suppressing the peripheral rods using a dim background, or using a using a very small five degree dim stimulus that produced no recordable scattered light component (Binns, & Margrain 2006; Choshi et al., 2003; Hood et al., 1998). While rod-isolated focal ERG responses can be obtained by these methods, the b-wave responses recorded are extremely small (<10 μV).

Nusinowitz et al (1995) described a method for deriving focal rod-isolated ERG a-waves from a 40 degree field centered on the macula. The technique used bright paired flashes. The first bright flash triggers a response from local rods and cones in the central 40 degree field, as well as from peripheral photoreceptors due to scattered light. The second flash, given while central rods are still saturated from the first flash, triggers a response from cones and peripheral rods, but not central, rods. The rod-isolated ERG response from the central 40 degree field, is obtained by subtracting the second flash response from the that of the first. Relatively large focal rod ERG a-waves, with peak a-wave amplitude of some 40 μV were obtained using this paired flash method. Nusinowitz et al (1995) was also able to fit a P3 model to these central rod a-waves, thereby providing a quantitative description of central rod phototransduction. However, to achieve the alignment necessary for their technique, Nusinowitz et al (1995) used Maxwellian view projection, a method not amenable to use with anesthetized animals.

Here we adapt the method described by Nusinowitz et al (1995) to enable measurement of rod phototransduction from the central retina of the anesthetized monkey using a standard Ganzfeld stimulus. The results demonstrate a selective reduction in central rod function that worsens with age in a group of Japanese macaques with dominant drusen. By comparison there was no effect of drusen in these macaques on the kinetics of dark adaptation measured with the full field bright flash ERG.

2. Experimental methods and results

2.1 Animals

All experiments were reviewed and approved by the Institutional Animal Care and Use Committee of the Oregon National Primate Research Center and were conducted in accordance with the ARVO statement for the Use of Animals in Ophthalmic and Vision Research.

Color retinal fundus photography was used to screen for retinal phenotypes in a troop of Japanese macaques (Macaca fuscata) resident at the Oregon National Primate Research Center since 1964. Selected macaques were also assessed by fluorescein angiography. We identified a distinct retinal disease syndrome in these macaques that is characterized by dominant inheritance and the early onset of pan-retinal drusen (Neuringer M, et al. IOVS 2011;52:ARVO E-Abstract 4008). Electroretinograms (ERGs) were recorded from eight of these Japanese macaques that were aged between 6 and 27 years at the time of testing. Four monkeys had no evidence of drusen, while the other 4 monkeys had severe drusen noted on retinal fundus photographs and fluroscein angiograms.

2.2 Animal preparation

In preparation for ERG recording, monkeys were anesthetized with intramuscular injection of ketamine (10 mg/kg), xylazine (1.0 mg/kg) and atropine (0.4 mg/kg). Anesthesia was maintained with ketamine (5 mg/kg), xylazine (0.5 mg/kg) and atropine (0.4 mg/kg) at 30- to 50-minute intervals as required. Ketamine and atropine were administered at least five minutes before xylazine injection. Supplemental oxygen was delivered via nasal canula at 0.5 liters/minute, and both the heart rate and oxygen saturation were monitored by pulse oximetry. Core body temperature was maintained between 37.0°C and 38.5°C by using water-circulated heated pads placed either side of the animal. After completion of the ERG studies, a triple antibiotic (Vetropolycin; Dechra Pharmaceuticals, Overland Park, KS) was placed on the eyes and an analgesic (ketaprofen, 20 mg/kg) given intramuscularly. Animals were recovered in a darkened room before being returned to their holding cage.

Before ERG recording, pupils were dilated to approximately 8 mm with phenylephrine (2.5%) and tropicamide (1%). The cornea was anesthetized with proparacaine (1%) and lubricated with methylcellulose (1%) before insertion of a bipolar Burian-Allen contact lens electrode (Hansen Ophthalmic Development Laboratory, Iowa City, IA). A subdermal needle electrode placed in the back served as ground. With the bright flash intensities used here, we often encountered large flash artifacts during ERG recording. We found that covering the silvered speculum of the Burian-Allen electrode with black ink from a permanent marker and placing a collar made from black plastic around the top edge of the speculum minimized such flash artifacts. Animals were dark adapted for 30 minutes prior to ERG recording. ERGs were amplified (10 000) and filtered (-3dB at 0.1Hz & 1 kHz) before being sampled at 5 kHz with a 12-bit A/D converter and stored for off-line analysis.

2.3 Light stimulation

Flash stimulation was provided by two high-intensity photoflash units (2405CX and a modified 1205 CX power supplies with 205 flash units: Speedotron; Chicago, Ill) mounted on a customized 35-cm Ganzfeld. Flash intensities in candela-seconds/metre^2 (cd-s/m^2) were measured by a photometer with a scotopic filter set to integration mode for measurement of brief flashes (PR1980A-PL, Photo Research, Chatsworth CA). Retinal illuminance in scotopic trolands (sc Td-s) was calculated from the respective flash energies and pupil size (Wyszecki, & Stiles 1982).

2.4 Method for measuring full field rod phototransduction

The left columns of Figures 1 & 2 outline the paired flash protocol (Birch, & Hood 1995) used to derive full-field rod isolated ERG a-waves. Full-field ERG rod a-waves were

recorded to flash intensities of 2.1 - 4.5 log sc Td-s in approximately 0.3 log unit steps. ERGs to the first (test) flash contained both rod and cone contributions (Figure 1A). Isolating the cone contributions to these ERGs required a differential approach that depended on first flash intensity. For test flash intensities greater than 3.3 log sc Td-s, rods saturate for longer

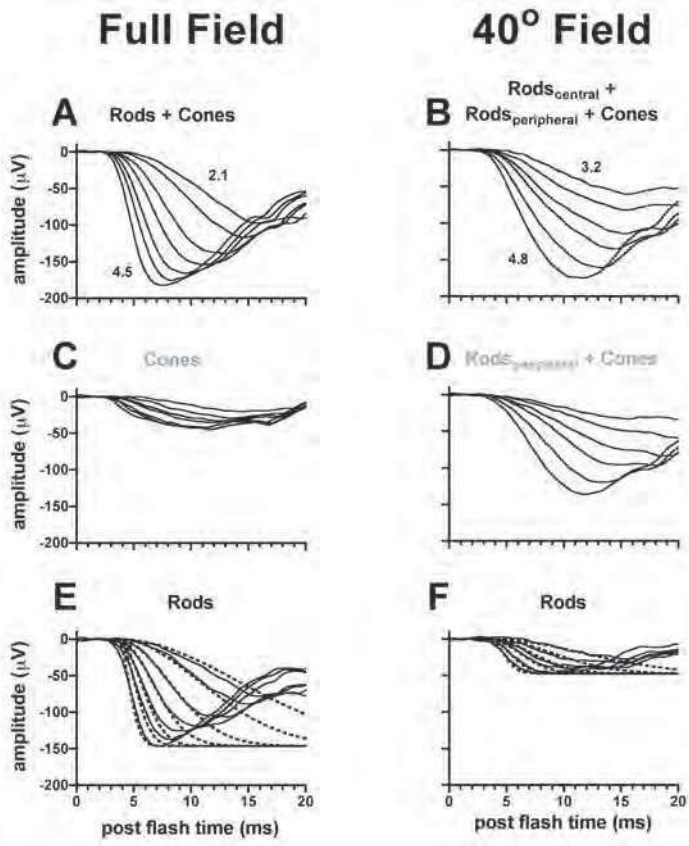

Fig. 1. Derivation of full- and restricted -field rod ERG a-waves. **Left column: A.** Mixed rod/cone ERG a-waves to a range of flash intensities (2.1 - 4.5 log sc Td-s) in response to the first flash of paired-flash paradigm. **C.** Cone ERG a-waves to the same flash intensities in response to the second of the paired flashes. **E.** Full-field rod-isolated ERG a-waves obtained by subtracting response in C from those in A. Dashed lines show the ensemble fit of the P3 model (eqn 1) to the leading edges of the ERG a-waves. For this 27 year old monkey, $Rmax_{P3}$ = -146 μV, S = (16.2 sc Td-s)$^{-1}$ s^{-2}, td = 3.6 ms. **Right column: B.** Mixed rod/cone ERG a-waves to a range of flash intensities (3.2 - 4.8 log sc Td-s) in response to an isolated flash. **D.** The cone and scattered rod contributions are calculated from the same flashes presented 2.2 sec after a 3.3 log sc Td-s conditioning flash. **F.** Rod-isolated ERG a-waves from the central 40° obtained by subtracting responses in D from those in B. Dashed lines show the ensemble fit of the P3 model (eqn 1) to the leading edges of the ERG a-waves.For this 27 year old monkey, $Rmax_{P3}$ = -47 μV, S = (5.1 sc Td-s)$^{-1}$ s^{-2}, t_d=3.5 ms

than 1.5 seconds, but cones recover in less than 400 milliseconds (unpublished data). Therefore, dark adapted cone ERGs were obtained by presenting two identical flashes separated by an interstimulus interval (ISI) of one second (Figure 2B). Thus, the second flash was presented while the rods were still saturated from the first flash. For retinal illuminances under 3.3 log scot Td-s, rods did not saturate for sufficient time to allow direct application of this paired flash method. Instead a two step process was necessary (Figure 2A). In the first step, ERGs were recorded to isolated test flashes (Figure 2A). In the second step, the ERG was then recorded to these same test flashes, presented 1 second after a 3.3 log sc Td-s conditioning flash (Figure 2A). This 1.0 sec interval ensured that the test flash occurred after complete cone recovery but before the onset of rod recovery from the conditioning flash. Figure 1C shows the full-field cone ERGs obtained using this differential approach. Rod isolated ERG a-waves (Figure 1E) were obtained by subtracting the dark-adapted cone-isolated ERGs (Figure 1C) from the mixed rod/cone responses (Figure 1A).

2.5 Method of rod phototransduction analysis

Rod phototransduction was quantified from the fit of the following P3 model to the leading edges the rod-isolated ERG a-waves (Birch et al., 1995):

$$P3\ (i, t) \cong [1 - \exp(-I \bullet S \bullet (t - t_d)^2)] \bullet Rmax_{P3}\ t > td \quad (1)$$

where P3 is the leading edge of the a-wave at time (t) seconds, in response to a flash with a retinal illuminance of I (sc Td-s). The parameters derived to fit the model were: S ((sc Td-s)$^{-1}$ s^{-2}), the sensitivity parameter that scales retinal illuminance; t_d (secs), the delay due to the filter and finite duration of the flash; and $Rmax_{P3}$ (μV) , the maximum rod photoresponse .

The parameters of the P3 model were determined by fitting equation 1 simultaneously (ensemble fit) to the leading edges of the of the ERG a-waves for retinal illuminances from 2.4 to 4.2 log scot Td-s . The "leading edge" of the ERG a-wave for each flash intensity was determined to be all points with amplitude less than 80% of the a-wave peak. The 80% value was chosen to avoid the influence of the post-receptoral components that contribute to the a-wave near its peak (Robson et al., 2003). During fitting, $Rmax_{P3}$ was fixed at the maximal a-wave amplitude obtained and S and t_d were varied. All analysis was performed with custom written Matlab programs (David Birch, Retina Foundation of the Southwest, Dallas, TX.).

In Figure 1C, the fit of the P3 model (dotted lines) provides a good description of the rising phases to the ERG a-waves for all but the two highest intensities where rate saturation becomes a limiting factor (Breton et al., 1994; Lamb et al., 1992).

2.6 Method for measuring restricted field rod phototransduction

The right columns of Figures 1 & 2 outline the protocol used to derive rod isolated ERG a-waves from a 40 degree field centered on the macula (Nusinowitz et al., 1995). The restricted field ERG protocol also makes used of the paired flash method, but requires two recording steps (Figure 2 C). In the first step, the ERG is recorded to an isolated test flash (3.2 - 4.8 log sc Td-s) presented over a 40 degree field centered on the macula (Figure 2C). The ERG response ERG_{total} to this isolated test flash (Figure 1B), contains rod and cone components from the central 40 degree field as well as rod and cone components from the peripheral retina generated by scattered light (Nusinowitz et al., 1995).; i.e.

$$ERG_{total} = Rods_{central} + Cones_{central} + Rods_{peripheral} + Cones_{perpipheral} \quad (2a)$$

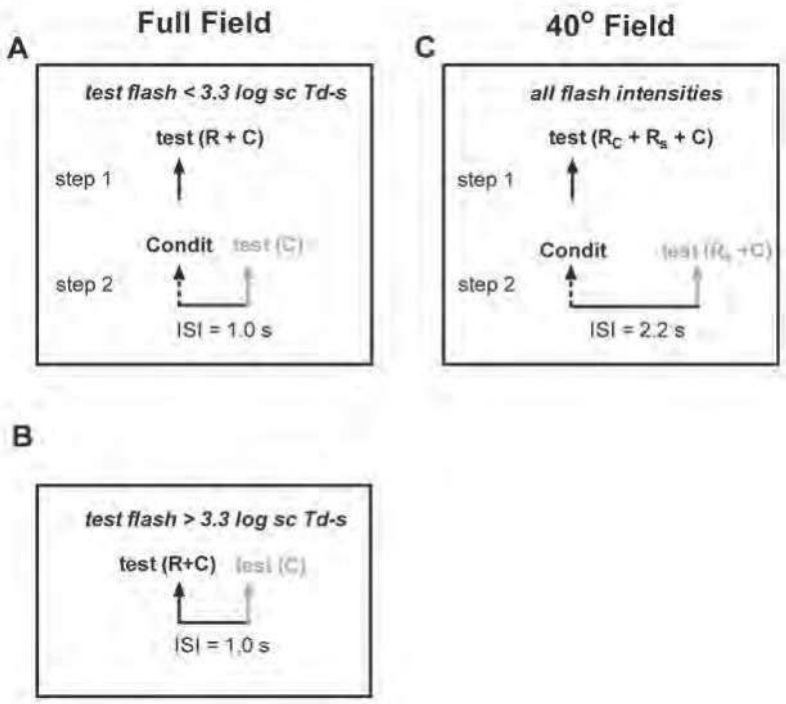

Fig. 2. Graphical representation of stimuli timing for rod phototransduction.**A.** Derivation of full-field rod-isolated ERG a-wave requires two steps for test flash intensities < 3.3 log sc Td-s. Isolated test flashes (step 1) contain both rod and cone (R+C) contributions. Step 2: The interstimulus interval (ISI) between the conditioning flash (3.3 log sc Td-s) and test flash was set to 1.0 sec. With this ISI, the ERG to the test flash contains only cone contributions. **B.** For test flash intensities above 3.3 log sc Td-s, ERGs are recorded to identical flashes separated by an ISI of 1.0 sec. **C.** Step 1: the test flashes presented in isolation in a 40º field centered on the macula contain rod and cone contributions from the central retina ($R_c + C_c$) and from the peripheral retina ($R_p + C_p$). Step 2: When presented 2.2 sec after a 4.4 log sc Td-s conditioning flash, ERG recorded to the test flashes contain central and peripheral cone contributions and peripheral rod contributions (see main text).

In the second recording step, the same test flash intensities from step 1 are each presented 2.2 sec after a 4.4 log sc Td-s conditioning flash (Figure 1C) that saturates central rods for >2.4 sec (Jeffrey et al., 2002; Jeffrey, & Neuringer 2009). Cones recover in less than 0.4 sec to this conditioning flash intensity (unpublished data). The intensity of the scattered light is estimated to be 1.5 - 2.0 log units dimmer than the conditioning flash, i.e. scattered light intensity in the peripheral retina ranges from 2.4 - 2.9 log sc Td-s (Nusinowitz et al., 1995). At theses flash intensities, rods achieve greater than 90% recovery 2.2 sec after a flash (Jeffrey, & Neuringer 2009). Therefore, ERGs recorded to the test flash presented 2.2 sec after a conditioning flash, do not contain any rod responses from the central retina. However, by 2.2 sec, the central cones and peripheral photoreceptor responses will have fully recovered.

Thus, the ERG response to a test flash presented 2.2 sec after the conditioning flash (Figure 1D) will be:

$$ERG_{test} = Cones_{central} + Rods_{peripheral} + Cones_{perpipheral} \quad (2\,b)$$

The final step to isolating the rod ERG a-wave from the central 40 degree is to subtract the ERGs recorded in step 2 (eqn 2b) from the total ERG response recorded to the same flash intensities in step 1 (eqn 2a). i.e.

$$Rods_{central} = ERG_{total} - ERG_{test} \quad (2c)$$

Figure 1F shows the rod-isolated ERG a-waves from a 40 degree field centered on the macula of a 27 year old monkey.

For the restricted field ERG, the P3 model was fit to the leading edges of the ERG a-waves for retinal illuminances from 3.5 to 4.8 log sc Td-s. The range of retinal illuminances for the restricted field analysis, which was higher than the intensity range used for the full-field, was necessary due to the lower sensitivity obtained from the rods in the central visual field (see section 2.7 below).

2.7 Results: full- and restricted-field phototransduction

We examined whether rod phototransduction was altered in eight Japanese macaques that either had no or only mild central drusen (n=4; mean age ± SE = 11.8 ± 2.3 years) or severe drusen (n=4; mean age ± SE = 16.3 ± 4.1 years). Rod phototransduction parameters were compared using a 2-way ANOVA for the main effects of drusen and field size. There were

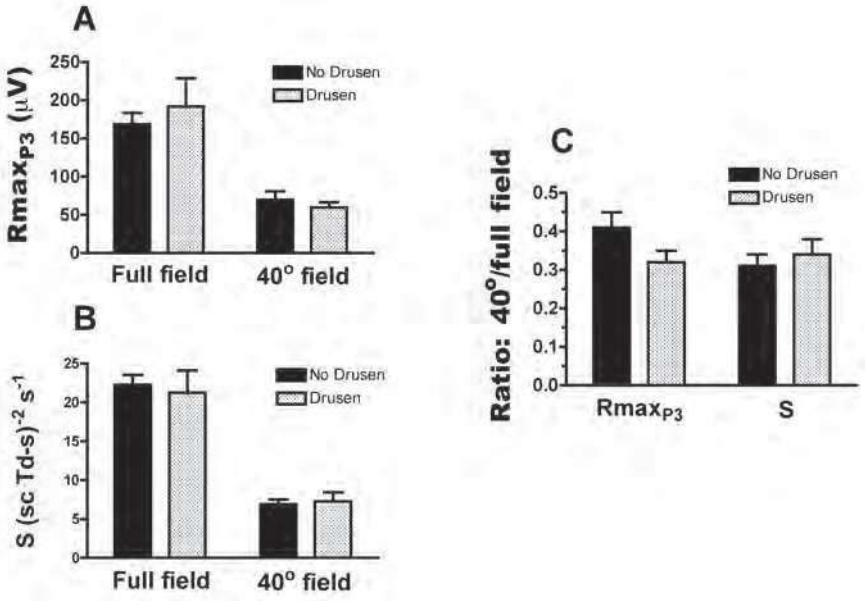

Fig. 3. Mean phototransduction parameters by drusen group. Mean rod maximal responses, Rmax$_{P3}$ (**A**) and sensitivities S (**B**) for drusen and no drusen monkeys for both full- and 40^{o}-fields. **C**. Ratio of 40^{o} to full field values for Rmax$_{P3}$ and S.

no significant differences between drusen and no drusen monkeys for the absolute values of maximal rod response, $Rmax_{P3}$ (Figure 3A) nor for rod sensitivity, S (Figure 3B). For both $Rmax_{P3}$ and S, there was a significant effect of field size ($p<0.0001$). For all monkeys combined, $Rmax_{P3}$ from the central 40 degree field (mean ± SE = -65.4 ± 6.7 μV) was reduced by 63 % in comparison with the mean full field value (-178.6 ± 16.7 μV). Similarly rod sensitivity from the central retina (7.1 ± 0.6 [sc Td-s]$^{-1}$ s $^{-2}$) was reduced 68 % compared with full field values (21.8 ± 1.3 [sc Td-s]$^{-1}$ s $^{-2}$) . Overall monkeys with severe drusen had greater variability for both full- and restricted field values of $Rmax_{P3}$ and S (Figures 3A & B).

While absolute values of rod phototransduction were not different between drusen and no drusen monkeys, we wanted to examine whether there may be selective loss of central rod function in monkeys with drusen. To this end, we calculated the ratio of the 40 deg to full field values for each of the rod phototransduction parameters. Calculating this ratio negates the inherent variability in absolute amplitude measures, and enables the central retina to be normalized with respect to the whole retina for each animal. Figure 3C shows a trend for a reduction in the 40^{o}/full field ratio of $Rmax_{P3}$ from the drusen monkeys, although the difference did not reach significance ($p=0.13$). This reduction in the 40^{o}/full field $Rmax_{P3}$ ratio suggests a selective loss of central rod function in drusen monkeys compared with the no drusen monkeys. There was no difference in the 40^{o}/full field S ratio between the drusen and no drusen groups (Figure 3C).

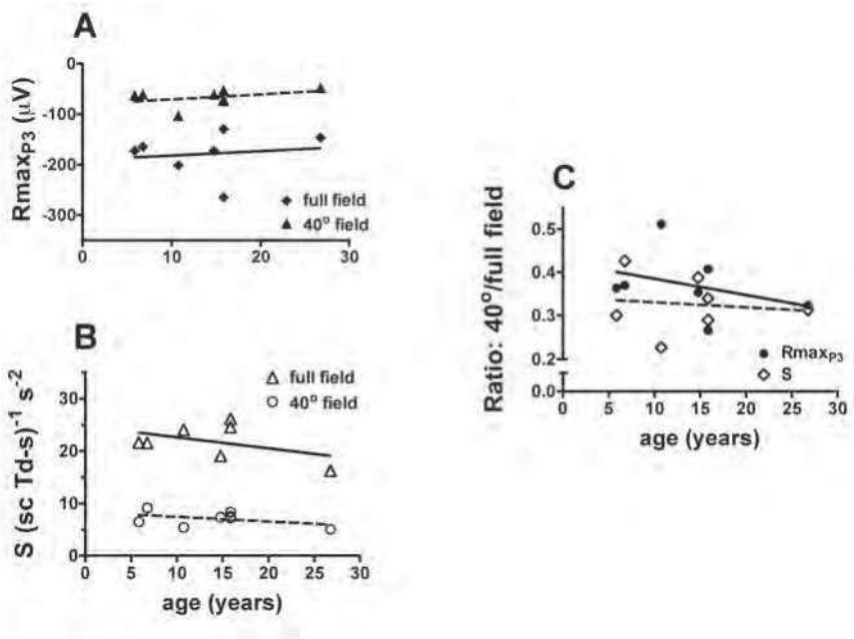

Fig. 4. Variation in phototransduction parameters with age.Rod maximal amplitude, $Rmax_{P3}$ (**A**) and rod sensitivity S (**B**) plotted as a function of age for both full- and 40^{o}-fields. Solid lines: 40^{o} field, dashed lines: full field. **C**. Ratio of 40^{o} to full field values for $Rmax_{P3}$ and S plotted as a function of age. Solid line: $Rmax_{P3}$, dashed line: S.

We also examined the effect of age on rod phototransduction parameters. There were general trends for inverse relationships between both $Rmax_{P3}$ (Figure 4A) and S (Figure 4B) with age. Note that since $Rmax_{P3}$ is plotted as a negative voltage, an inverse relationship for amplitude (Figure 4A) will be in the opposite direction to the same relationship for S (Figure 4B). Figure 4C shows the plots of 40°/full field ratios for $Rmax_{P3,}$ and S as a function of age. The negative slope of the 40°/full field $Rmax_{P3}$ ratio with age (Figure 4C; solid symbols, solid line) suggests a selective loss of central rod function with increasing age in these Japanese macaques.

2.8 Dark adaptation: ERG recording methods and analysis

The left column of Figure 5 outlines the paired flash protocol used to quantify the kinetics of dark adaptation as measured from the recovery of rod-isolated ERG a-wave amplitude following a bleach. In order to bleach greater than 99% of all retinal pigment, one eye of the monkey was exposed to a yellow background with retinal illuminance of 15 000 cd/m^2 for two minutes (Thomas, & Lamb 1999). To obtain the background intensity necessary for a full bleach, we built a six cm mini-ganzfeld that was connected to an incandescent light

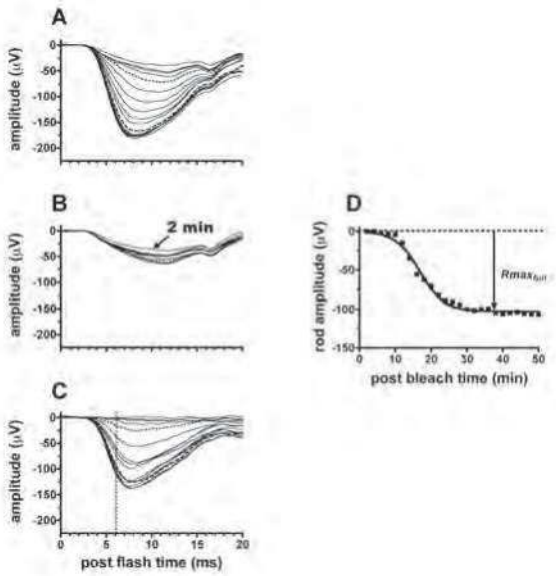

Fig. 5. Derivation of full-field dark adaptation. **A.** Recovery of ERG a-wave amplitude to a 4.4 log sc Td-s flash over a 50 minute period following a >99% bleach. All ERG's recorded over the first 20 min are shown; at longer post-bleach times, every other ERG recorded (i.e. 4 min separation) is shown. Responses at 10 and 24 min post-bleach are indicated by the dotted and dashed lines respectively. All ERGs contain mixed rod and cone contributions. **B.** Cone isolated ERG a-waves to an identical flash (4.4 log sc Td-s) for the same post bleach times shown in A. **C.** Full-field rod-isolated ERG a-waves obtained by subtracting the cone responses in B from the mixed rod/cone responses in A. Vertical dotted line indicates the time (6 ms post flash) at which rod ERG a-wave amplitude was measured. **D.** Rod isolated ERG a-wave amplitude plotted as a function of time post bleach. The solid line, shows the plot of equation 3. For this 27 year old monkey, $Rmax_{P3}$ = -103 μV, c_a = 146, τ_{DA} = 3.4 min.

source through a filter box via two fiber optic cables. Following the full bleach, scotopic full-field ERGs were recorded to paired identical flashes (4.4 log sc Td-s flash, ISI = 1.0 sec) every two minutes for 50 minutes. The technique for isolating the rod ERG a-wave is essentially identical to the method used above (Section 2.4) for assessing full field rod phototransduction. Figure 5A shows the mixed rod/cone ERG responses recorded to the first flash and Figure 5B corresponding cone isolated responses obtained from the second flash of the pair. Rod isolated ERG a-waves (Figure 5C) were then obtained by subtracting a dark-adapted cone-isolated ERGs (Figure 5B) from the mixed rod/cone responses (Figure 5A). Rod ERG a-wave amplitude was measured at 6 millisecond post flash (Figure 5C: vertical dotted line) to avoid contamination by post-receptoral components that may be present at the a-wave peak (Robson et al., 2003). Figure 5D shows the recovery of rod-isolated full-field rod ERG a-wave amplitude plotted as a function of post-bleach time. The recovery of ERG a-wave amplitude was well described by the following equation (Thomas, & Lamb 1999):

$$Rmax(T) = Rmax()/[\,1 + c_a \bullet \exp(-T/\tau_{DA})] \quad (3)$$

where Rmax(T) is the ERG a-wave amplitude (μV) at post-bleach time T (min) and Rmax() = ERG a-wave amplitude (μV) in the fully dark adapted retina. Derived parameters were c_a (no units) which describes the degree of reduction immediately after a bleach, and τ_{DA} (minutes) is the time constant of recovery of ERG a-wave amplitude.

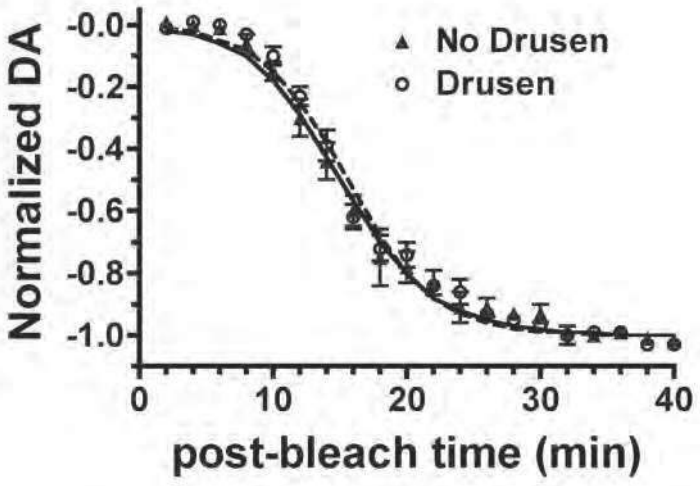

Fig. 6. Mean normalized dark adaptation by drusen group. Plot of mean normalized dark adaptation for the no drusen (solid squares) and drusen (open circles) monkeys plotted as a function of time. Solid and dashed lines show the mean fits of (eqn 3) for the no drusen and drusen groups, respectively.

Figure 5D shows that rod recovery began around 10 minutes post bleach and was almost complete by 24 minutes. The ERG responses at 10 and 24 minutes post-bleach are indicated by the dotted and dashed lines respectively in Figures 5 A-C. The cone response recorded 2

minutes post bleach (Figure 5B) was consistently smaller than all remaining cone ERGs. This was true for all monkeys in this study and indicates that cone recovery following a full bleach takes up to four minutes, similar to that reported for the human (Mahroo, & Lamb 2004) .
Figure 6 shows kinetics of dark adaptation were not different between the drusen and no drusen monkeys. For all monkeys combined, the time constant of dark adaptation was 3.1 ± 0.1 minutes (mean ± SE) and ERG a-wave amplitude had reached >97% of the full dark-adapted value within 28 minutes after a full bleach. These results in the Japanese macaque are similar to those obtained for humans using a similar ERG protocol (Thomas, & Lamb 1999).

3. Conclusion

In a unique colony of Japanese macaques at the Oregon National Primate Research Center we identified a distinct retinal disease characterized by dominant inheritance and the early onset of pan-retinal drusen syndrome (Neuringer M, et al. IOVS 2011;52:ARVO E-Abstract 4008). Although only a small number of these animals were available for functional testing, the ERG data presented in this report point to changes in the function of the central rods of these monkeys. The reduction in the 40^{o}/full field ratio for $Rmax_{P3}$ in the drusen monkeys suggests that the drusen in these animals is associated with selective changes in their central rod function. An alternative interpretation would be that selective loss of central $Rmax_{P3}$ may purely be a function of age based on the observed inverse correlation of 40^{o}/full field $Rmax_{P3}$ ratio with age, which was independent of drusen status. Monkeys in the drusen group were older (mean ± SE) at 16.3 ± 4.1 years than the no-drusen monkeys at 11.8 ± 2.3 years, although the difference did not reach significance. Regardless of the cause (drusen/age), the reduction in the 40^{o}/full field ratio for $Rmax_{P3}$ strongly suggests selective dysfunction or loss of rods from central retina of these Japanese macaques. Given these two results, a larger study will be required to determine if drusen status and/or age account for the loss of rod response from the central retina of this unique group of macaques.
Apart from drusen, these animals have no other overt signs of retinal disease. Therefore, the results presented in this study highlight that restricted field ERG measure of phototransduction may provide an objective and robust means to detect early pre-clinical signs of retinal dysfunction prior to the presence of more advances stages of age-related retinal disease.
This group of Japanese macaques with early onset dominantly inherited drusen adds to and complements other large scale studies in cynomologus and rhesus macaques that have reported drusen, with similar phenotype and genotypic characteristics to those observed with human drusen/early AMD. These non-human primate models of early AMD will prove invaluable as a resource for studying both the molecular and genetic mechanisms associated with the development of early AMD. In addition non-human primate models, especially those with early onset drusen, will likely provide an invaluable resource for preclinical testing of AMD therapies. Although rodent models can provide information regarding some of the processes underlying macular degeneration in AMD, non-human primates are the only animals with a retina essentially identical to that of the human. Only monkeys, apes and humans have nearly identical retinal structure including the presence of a macula and a foveal pit with high cone density and adjacent peak RPE cell density. Lastly, rodents do not accumulate significant xanthophylls in the retina, whereas a defining characteristic of the primate macula is the presence of the xanthophylls lutein and zeaxanthin.

4. Acknowledgment

Funded in part by American Health Assistance Foundation's Macular Degeneration Research Program; The Foundation Fighting Blindness, Research to Prevent Blindness and National Institutes of Health grant RR00163. We thank David Birch PhD (Retina Foundation of the Southwest, Dallas Tx) for the Matlab routines used for fitting the P3 model to the ERG a-waves for assessment of rod phototransduction. We thank Lauren Renner BSc for assistance with ERG recording and animal care.

5. References

Berrow, E.J., Bartlett, H.E., Eperjesi, F. & Gibson, J.M., 2010, The electroretinogram: a useful tool for evaluating age-related macular disease? *Documenta ophthalmologica. Advances in ophthalmology*, 121(1), pp. 51-62.

Binns, A. & Margrain, T.H., 2006, Development of a technique for recording the focal rod ERG, *Ophthalmic & physiological optics* 26(1), pp. 71-9.

Binns, A.M. & Margrain, T.H., 2007, Evaluating retinal function in age-related maculopathy with the ERG photostress test, *Investigative ophthalmology & visual science*, 48(6), pp. 2806-13.

Birch, D.G. & Hood, D.C. 1995, Abnormal rod photoreceptor function in Retinitis Pigmentosa, in RE Anderson (ed), *Degenerative diseases of the Retina,* Plenum Press, New York, pp. 359-69.

Birch, D.G., Hood, D.C., Nusinowitz, S. & Pepperberg, D.R., 1995, Abnormal activation and inactivation mechanisms of rod transduction in patients with autosomal dominant retinitis pigmentosa and the pro-23-his mutation, *Investigative Ophthalmology and Visual Science*, 36(8), pp. 1603-14.

Bonilha, V.L., 2008, Age and disease-related structural changes in the retinal pigment epithelium, *Clinical ophthalmology* , 2(2), pp. 413-24.

Breton, M.E., Schueller, A.W., Lamb, T.D., Pugh, E.N. & Jr., 1994, Analysis of ERG a-wave amplification and kinetics in terms of the G-protein cascade of phototransduction, *Investigative Ophthalmology and Visual Science*, 35(1), pp. 295-309.

Choshi, T., Matsumoto, C.S. & Nakatsuka, K., 2003, Rod-driven focal macular electroretinogram, *Japanese journal of ophthalmology*, 47(4), pp. 356-61.

Curcio, C.A., Medeiros, N.E. & Millican, C.L., 1996, Photoreceptor loss in age-related macular degeneration, *Investigative ophthalmology & visual science*, 37(7), pp. 1236-49.

Curcio, C.A., Millican, C.L., Allen, K.A. & Kalina, R.E., 1993, Aging of the human photoreceptor mosaic: evidence for selective vulnerability of rods in central retina, *Investigative ophthalmology & visual science*, 34(12), pp. 3278-96.

Curcio, C.A., Owsley, C. & Jackson, G.R., 2000, Spare the rods, save the cones in aging and age-related maculopathy, *Investigative ophthalmology & visual science*, 41(8), pp. 2015-8.

Curcio, C.A., Sloan, K.R., Kalina, R.E. & Hendrickson, A.E., 1990, Human photoreceptor topography, *Journal of Comparative Neurology*, 292(4), pp. 497-523.

Dawson, W.W., Dawson, J.C., Lake, K.P. & Gonzalez-Martinez, J., 2008, Maculas, monkeys, models, AMD and aging, *Vision research*, 48(3), pp. 360-5.

Eisner, A., Klein, M.L., Zilis, J.D. & Watkins, M.D., 1992, Visual function and the subsequent development of exudative age-related macular degeneration, *Investigative ophthalmology & visual science*, 33(11), pp. 3091-102.

Falsini, B., Serrao, S., Fadda, A., Iarossi, G., Porrello, G., Cocco, F. & Merendino, E., 1999, Focal electroretinograms and fundus appearance in nonexudative age-related

macular degeneration. Quantitative relationship between retinal morphology and function, *Graefe's archive for clinical and experimental ophthalmology*, 237(3), pp. 193-200.

Francis, P.J., Appukuttan, B., Simmons, E., Landauer, N., Stoddard, J., Hamon, S., Ott, J., Ferguson, B., Klein, M., Stout, J.T. & Neuringer, M., 2008, Rhesus monkeys and humans share common susceptibility genes for age-related macular disease, *Human molecular genetics*, 17(17), pp. 2673-80.

Gao, H. & Hollyfield, J.G., 1992, Aging of the human retina. Differential loss of neurons and retinal pigment epithelial cells, *Investigative ophthalmology & visual science*, 33(1), pp. 1-17.

Gerth, C., 2009, The role of the ERG in the diagnosis and treatment of Age-Related Macular Degeneration, *Documenta ophthalmologica. Advances in ophthalmology*, 118(1), pp. 63-8.

Gouras, P., Ivert, L., Mattison, J.A., Ingram, D.K. & Neuringer, M., 2008, Drusenoid maculopathy in rhesus monkeys: autofluorescence, lipofuscin and drusen pathogenesis, *Graefe's archive for clinical and experimental ophthalmology*, 246(10), pp. 1403-11.

Haegerstrom-Portnoy, G., 2005, The Glenn A. Fry Award Lecture 2003: Vision in elders--summary of findings of the SKI study, *Optometry and vision science* , 82(2), pp. 87-93.

Haimovici, R., Owens, S.L., Fitzke, F.W. & Bird, A.C., 2002, Dark adaptation in age-related macular degeneration: relationship to the fellow eye, *Graefe's archive for clinical and experimental ophthalmology*, 240(2), pp. 90-5.

Hogg, R.E. & Chakravarthy, U., 2006, Visual function and dysfunction in early and late age-related maculopathy, *Progress in retinal and eye research*, 25(3), pp. 249-76.

Holder, G.E., 2001, Pattern electroretinography (PERG) and an integrated approach to visual pathway diagnosis, *Progress in retinal and eye research*, 20(4), pp. 531-61.

Hood, D.C., Wladis, E.J., Shady, S., Holopigian, K., Li, J. & Seiple, W., 1998, Multifocal rod electroretinograms, *Investigative ophthalmology & visual science*, 39(7), pp. 1152-62.

Hope, G.M., Dawson, W.W., Engel, H.M., Ulshafer, R.J., Kessler, M.J. & Sherwood, M.B., 1992, A primate model for age related macular drusen, *The British journal of ophthalmology*, 76(1), pp. 11-6.

Jackson, G.R., McGwin, G., Phillips, J.M., Klein, R. & Owsley, C., 2006, Impact of aging and age-related maculopathy on inactivation of the a-wave of the rod-mediated electroretinogram, *Vision research*, 46(8-9), pp. 1422-31.

Jackson, G.R., Owsley, C. & Curcio, C.A., 2002, Photoreceptor degeneration and dysfunction in aging and age-related maculopathy, *Ageing research reviews*, 1(3), pp. 381-96.

Jackson, G.R., Owsley, C. & McGwin, G., 1999, Aging and dark adaptation, *Vision research*, 39(23), pp. 3975-82.

Jeffrey, B.G. & Neuringer, M., 2009, Age-Related Decline in Rod Phototransduction Sensitivity in Rhesus Monkeys Fed an n-3 Fatty Acid Deficient Diet, *Investigative ophthalmology & visual science*, 50(9), pp. 4360-7.

Jeffrey, B.G., Mitchell, D.C., Gibson, R.A. & Neuringer, M., 2002, n-3 fatty acid deficiency alters recovery of the rod photoresponse in rhesus monkeys, *Investigative ophthalmology & visual science*, 43(8), pp. 2806-14.

Lamb, T.D., Pugh, E.N. & Jr., 1992, A quantitative account of the activation steps involved in phototransduction in amphibian photoreceptors, *Journal of Physiology (Lond)*, 449, pp. 719-58.

Mahroo, O.A. & Lamb, T.D., 2004, Recovery of the human photopic electroretinogram after bleaching exposures: estimation of pigment regeneration kinetics, *The Journal of physiology*, 554(Pt 2), pp. 417-37.

Morrison, J.D. & McGrath, C., 1985, Assessment of the optical contributions to the age-related deterioration in vision, *Quarterly journal of experimental physiology*, 70(2), pp. 249-69.

Neelam, K., Nolan, J., Chakravarthy, U. & Beatty, S., 2009, Psychophysical function in age-related maculopathy, *Survey of ophthalmology*, 54(2), pp. 167-210.

Nusinowitz, S., Hood, D.C. & Birch, D.G., 1995, Rod transduction parameters from the a wave of local receptor populations, *Journal Optical Society America A*, 12(10), pp. 2259-66.

Owsley, C., Jackson, G.R., White, M., Feist, R. & Edwards, D., 2001, Delays in rod-mediated dark adaptation in early age-related maculopathy, *Ophthalmology*, 108(7), pp. 1196-202.

Packer, O., Hendrickson, A.E. & Curcio, C.A., 1989, Photoreceptor topography of the retina in the adult pigtail macaque (Macaca nemestrina), *Journal of Comparative Neurology*, 288(1), pp. 165-83.

Phipps, J.A., Guymer, R.H. & Vingrys, A.J., 2003, Loss of cone function in age-related maculopathy, *Investigative ophthalmology & visual science*, 44(5), pp. 2277-83.

Robson, J.G., Saszik, S.M., Ahmed, J. & Frishman, L.J., 2003, Rod and cone contributions to the a-wave of the electroretinogram of the macaque, *The Journal of physiology*, 547(Pt 2), pp. 509-30.

Sandberg, M.A., Pawlyk, B.S. & Berson, E.L., 1996, Isolation of focal rod electroretinograms from the dark-adapted human eye, *Investigative ophthalmology & visual science*, 37(5), pp. 930-4.

Shelley, E.J., Madigan, M.C., Natoli, R., Penfold, P.L. & Provis, J.M., 2009, Cone degeneration in aging and age-related macular degeneration, *Archives of ophthalmology*, 127(4), pp. 483-92.

Singh, K.K., Krawczak, M., Dawson, W.W. & Schmidtke, J., 2009, Association of HTRA1 and ARMS2 gene variation with drusen formation in rhesus macaques, *Experimental eye research*, 88(3), pp. 479-82.

Snodderly, D.M., Auran, J.D. & Delori, F.C., 1984, The macular pigment. II. Spatial distribution in primate retinas, *Investigative ophthalmology & visual science*, 25(6), pp. 674-85.

Spear, P.D., 1993, Neural bases of visual deficits during aging, *Vision research*, 33(18), pp. 2589-609.

Thomas, M.M. & Lamb, T., 1999, Light adaptation and dark adaptation of human rod photoreceptors measured from the a-wave of the human electroretinogram, *Journal of Physiology*, 518, pp. 479-96.

Umeda, S., Ayyagari, R., Suzuki, M.T., Ono, F., Iwata, F., Fujiki, K., Kanai, A., Takada, Y., Yoshikawa, Y., Tanaka, Y. & Iwata, T., 2003, Molecular cloning of ELOVL4 gene from cynomolgus monkey (Macaca fascicularis), *Experimental animals / Japanese Association for Laboratory Animal Science*, 52(2), pp. 129-35.

Umeda S, Ayyagari R, Allikmets R, Suzuki MT, Karoukis AJ, Ambasudhan R, Zernant J, Okamoto, H., Ono, F., Terao, Mizota, A Yoshikawa Y, Tanaka Y Iwata, T. K., 2005a Early-onset macular degeneration with drusen in a cynomolgus monkey (Macaca fascicularis) pedigree: exclusion of 13 candidate genes and loci. *Investigative ophthalmology & visual science* 46, pp. 683-691.

Umeda, S., Suzuki, M.T., Okamoto, H., Ono, F., Mizota, A., Terao, K., Yoshikawa, Y., Tanaka, Y. & Iwata, T., 2005b, Molecular composition of drusen and possible involvement of anti-retinal autoimmunity in two different forms of macular degeneration in cynomolgus monkey (Macaca fascicularis), *The FASEB journal*, 19(12), pp. 1683-5.

Wang, Y.-Z., 2001, Effects of aging on shape discrimination, *Optometry & Vision Science*, 78(6), pp. 447-54.

Wikler, K.C., Williams, R.W. & Rakic, P., 1990, Photoreceptor mosaic: number and distribution of rods and cones in the rhesus monkey retina, *Journal of Comparative Neurology*, 297(4), pp. 499-508.

Wyszecki, G. & Stiles, W.S., 1982, *Color Science: Concepts and methods, quantitative data and formulae,* 2nd ed. John Wiley & Sons, New York.

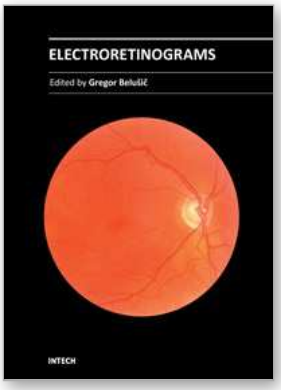

Electroretinograms

Edited by Dr. Gregor Belusic

ISBN 978-953-307-383-5
Hard cover, 238 pages
Publisher InTech
Published online 09, August, 2011
Published in print edition August, 2011

Electroretinography (ERG) is a non-invasive electrophysiological method which provides objective information about the function of the retina. Advanced ERG allows to assay the different types of retinal receptors and neurons in human and animal models. This book presents contributions on the recent state of the ERG. The book is divided into three parts. The first, methodological part, reviews standard methods and normatives of human ERG, reports about the advanced spatial, temporal and spectral methods of stimulation in human ERG, and deals with the analysis of the multifocal ERG signal. The second part deals with the ERG in different diseases of the human visual system and in diabetes. The third part presents the ERG in the standard animal models of human retinal disease: mouse, rat, macaque and fruitfly.

InTech Europe
University Campus STeP Ri
Slavka Krautzeka 83/A
51000 Rijeka, Croatia
Phone: +385 (51) 770 447
Fax: +385 (51) 686 166
www.intechopen.com

InTech China
Unit 405, Office Block, Hotel Equatorial Shanghai
No.65, Yan An Road (West), Shanghai, 200040, China
中国上海市延安西路65号上海国际贵都大饭店办公楼405单元
Phone: +86-21-62489820
Fax: +86-21-62489821